JOURNAL OF VIROLOGY, Nov. 1998, p. 8605–8612 Vol. 72, No. 11
0022-538X/98/$04.00+0

A Protein Critical for a Theiler's Virus-Induced Immune System-Mediated Demyelinating Disease Has a Cell Type-Specific Antiapoptotic Effect and a Key Role in Virus Persistence

GHANASHYAM D. GHADGE, LI MA, SHIGERU SATO, JONG KIM, AND RAYMOND P. ROOS*

Department of Neurology, The University of Chicago, Chicago, Illinois 60637

Received 16 March 1998/Accepted 8 July 1998

TO subgroup strains of Theiler's murine encephalomyelitis virus (TMEV) induce a persistent central nervous system infection and demyelinating disease in mice. This disease serves as an experimental model of multiple sclerosis (MS) because the two diseases have similar inflammatory white matter pathologies and because the immune system appears to mediate demyelination in both processes. We previously reported (H. H. Chen, W. P. Wong, L. Zhang, P. L. Ward, and R. P. Roos, Nat. Med. 1:927–931, 1995) that TO subgroup strains use an alternative initiation codon (in addition to the AUG used to synthesize the picornavirus polyprotein from one long open reading frame) to translate L*, a novel protein that is out of frame with the polyprotein and which plays a key role in the demyelinating disease. We now demonstrate that L* has antiapoptotic activity in macrophage cells and is critical for virus persistence. The antiapoptotic action of L* as well as the differential translation of L* and virion capsid proteins may foster virus persistence in macrophages and interfere with virus clearance. The regulation of apoptotic activity in inflammatory cells may be important in the pathogenesis of TMEV-induced demyelinating disease as well as MS.

Multiple sclerosis (MS), a chronic demyelinating disease of unknown cause, is believed to have an immune pathogenesis that is influenced by the genetics of the host as well as the environment, perhaps through exposure to a virus infection. DA strain and other TO subgroup members of Theiler's murine encephalomyelitis virus (TMEV) induce a persistent central nervous system (CNS) infection and demyelinating disease in mice that serves as an experimental model of MS (for a review, see reference 32). The two diseases have similar inflammatory white matter pathologies, and in both processes the immune system appears to contribute to the demyelination. The identification of the molecular determinants of DA-induced disease may increase our understanding of the pathogenesis of MS. We previously described a novel protein called L* that is synthesized by the demyelinating strains of TMEV and plays a key role in the white matter disease (7, 15). The present study shows that this protein has an antiapoptotic effect in macrophages and is critical for virus persistence.

Strains of TMEV, a murine cardiovirus, are divided into two subgroups on the basis of their markedly different biological activities in weanling mice. GDVII strain and other members of the GDVII subgroup of TMEV produce an acute fatal neuronal disease. In contrast, DA and other members of the TO subgroup of TMEV cause a biphasic disease with an initial subclinical neuronal infection followed by a chronic demyelinating process. The DA strain persists, with restricted expression (2, 4–6), in CNS glial cells (30) and microglia (16) for the life of the mouse.

As is the case with all picornaviruses, an internal ribosome entry site in the 5′ untranslated region of the TMEV genome enables ribosomes to bypass multiple AUGs (seven in the case of the DA strain) before initiating translation at the start of a long open reading frame (nucleotide [nt] 1066 in the case of the DA strain). The one long open reading frame is used for the synthesis of a polyprotein that is sequentially cleaved by proteases into structural and nonstructural proteins. At times, picornaviruses have an additional initiation codon, downstream of and in frame with the polyprotein's AUG, that is used in vitro (hepatitis A virus and encephalomyocarditis virus) or in vivo (foot-and-mouth disease virus) to synthesize a truncated polyprotein (13, 35, 38). The translation strategy of TO subgroup strains is uniquely different from that of other picornaviruses since these strains have an initiation codon (at nt 1079 in the case of DA), 13 nt downstream from the polyprotein's initiating AUG, that is used in vitro (15) and in vivo (7) to synthesize a 17-kDa protein called L* in a reading frame different from and overlapping that of the polyprotein (see the genome map in Fig. 1).

We initially suspected that L* might play a role in DA-induced disease since the nondemyelinating GDVII strains have an ACG rather than an AUG at the site corresponding to the alternative initiation codon for L* of DA and therefore do not synthesize L*. Our recent molecular genetic studies demonstrated that L* was, in fact, critical for the late demyelinating disease (7). These studies raised the possibility that ribosomes may initiate at either the polyprotein's AUG or the L* AUG, depending on the particular cell type, and that this variation may determine whether abundant virion capsid proteins are synthesized (leading to a productive and lytic infection) or whether there is a restrictive and persistent infection (with the synthesis of L* but few capsid proteins). The present study provides further characterization of the function of L* and its importance in virus persistence.

* Corresponding author. Mailing address: Department of Neurology (MC 2030), The University of Chicago, 5841 S. Maryland Ave., Chicago, IL 60637. Phone: (773) 702-6390. Fax: (773) 702-7775. E-mail: rroos@drugs.bsd.uchicago.edu.

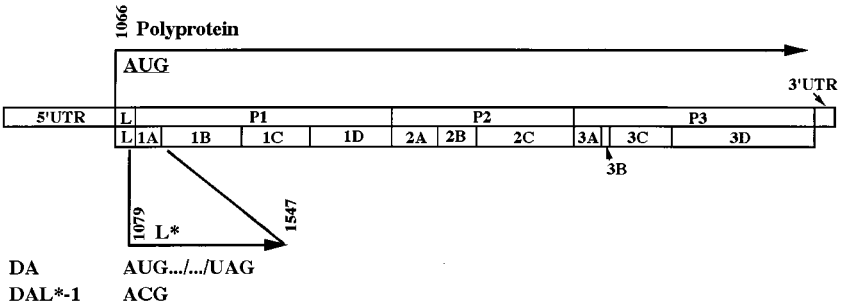

FIG. 1. Diagram of the viral genomes of wild-type DA and DAL*-1 viruses. The 5′ untranslated region (5′ UTR), the polyprotein coding region and its processing products, and the 3′ UTR are indicated. The initiation site for the polyprotein at nt 1066 and that for L* at nt 1079 (which is a reading frame different from that of the polyprotein) are shown, as is the stop UAG codon for L* at nt 1547. DAL*-1 virus has a C instead of a U at nt 1080 and fails to synthesize L*.

MATERIALS AND METHODS

Cells and viruses. BHK-21 cells (a baby hamster kidney cell line) and P388D1 cells (a mouse macrophage cell line) were obtained from the American Type Culture Collection and used for studies of virus growth and viral protein synthesis (see below). BHK-21 cells were grown on Dulbecco's modified Eagle medium containing 10% fetal bovine serum (FBS), 2 mM L-glutamine, and 0.01% gentamycin. P388D1 cells were propagated on RPMI 1640 medium containing 15% FBS, 2 mM L-glutamine, and 0.01% gentamycin. Virus stocks of wild-type DA, wild-type GDVII, and DAL*-1 viruses were respectively obtained following transfection into BHK-21 cells of transcripts derived in vitro from a full-length, infectious cDNA clone of a wild-type DA strain known as pDAFL3 (33), a wild-type full-length cDNA copy of a GDVII strain known as pGDFL2 (9), and a mutant pDAL*-1 construct in which the only difference from the wild-type DA virus genome is a mutation of the AUG at nt 1079 to ACG, which is used to synthesize L* (15) (see Fig. 1). This mutation in the DAL*-1 mutant virus abolishes the synthesis of L* but does not change the predicted amino acid sequence of the polyprotein.

In vitro virus growth cycle and infectivity assays. BHK-21 cells or P388D1 cells in 35-mm-diameter dishes were adsorbed in duplicate for 1 h with wild-type or mutant virus at a multiplicity of infection (MOI) of 10 PFU per cell. Monolayers were washed and scraped at various times postinfection (p.i.) and then assayed for infectivity on BHK-21 cells by a plaque assay.

Radiolabeling of infected cells. Plates (35-mm diameter) of cells were either mock infected or infected with wild-type or mutant virus at an MOI of 5 to 10 PFU per cell. After 1 h, the cells were washed twice with Hanks' balanced salt solution containing calcium, magnesium, and 2% FBS. Culture medium containing FBS (5% for BHK-21 and 10% for P388D1 cells) and actinomycin D (2 μg/ml) was added. One hour prior to addition of 50 μCi of [*trans*-^{35}S]methionine (ICN Biomedicals), the medium was replaced with methionine-free Dulbecco's modified Eagle medium containing one-third the original concentration of FBS. Cells were labeled with [^{35}S]methionine for various lengths of time and harvested after the radiolabeling period by lysis with 150 to 300 μl of sample buffer (50 mM Tris [pH 6.8], 2% sodium dodecyl sulfate [SDS], 0.1% bromophenol blue, 10% glycerol, and 350 mM β-mercaptoethanol). Radiolabeled proteins were separated by SDS–12.5% polyacrylamide gel electrophoresis and analyzed by autoradiography.

Assays of apoptosis. (i) DNA fragmentation analysis. Analysis of chromosomal DNA fragmentation was carried out as described by Bose et al. (3). Cells (0.5×10^6 to 1×10^6) were lysed in buffer (10 mM Tris [pH 7.5], 100 mM NaCl, 1 mM EDTA, 1% SDS, and 50 μg of proteinase K per ml) overnight at 43°C. The DNA was extracted with phenol followed by chloroform-isoamyl alcohol (24:1 [vol/vol] ratio) and then ethanol precipitated. Following centrifugation at 12,000 rpm in an Eppendorf centrifuge (model 5415C) at 4°C for 20 min, the DNA pellet was dissolved in 50 μl of TE (10 mM Tris [pH 8.0], 1 mM EDTA). The DNA was then analyzed by 2% agarose gel electrophoresis and stained with ethidium bromide.

(ii) TUNEL staining. Cells were either mock infected or infected with virus at an MOI of 5 and harvested at various time points. Cells were fixed in 4% formalin in phosphate-buffered saline for 10 min at room temperature. A 50-μl aliquot of the cell suspension was then dried on a microscope slide overnight. Apoptotic cells were detected by using an ApopTag in situ apoptosis kit (Oncor, Gaithersburg, Md.) in accordance with the manufacturer's instructions. For each virus infection of cells, a total of 40 to 100 cells were examined for terminal deoxynucleotidyltransferase-mediated dUTP-biotin nick end labeling (TUNEL) in randomized microscope fields from three to four coverslips. Statistical comparisons were made by using the Newman-Keuls test.

(iii) Hoechst 33342 staining. Hoechst 33342 staining was performed as previously described (12).

Animal studies. Weanling 3-week-old SJL/J mice (Jackson Laboratory) were inoculated intracerebrally with 0.03 ml of wild-type or DAL*-1 virus suspension. Animals were sacrificed 1 and 6 weeks postinoculation. The brain and spinal cord of each animal were removed and either frozen for analysis of the infectious virus and viral genome or fixed for pathological evaluation. Homogenates of frozen tissues from four randomly selected animals that had been inoculated 1 week previously with either wild-type or DAL*-1 virus were subjected to a plaque assay for determination of the presence of infectious virus. In addition, for detection of the viral genome as described below, RNA was extracted from the brain and spinal cord of each of two animals, inoculated with either wild-type or DAL*-1 virus, at both 1 and 6 weeks p.i. ($n = 8$ mice). Formalin-fixed, paraffin-embedded sections of spinal cord from five animals that had been inoculated with wild-type or DAL*-1 virus 1 and 6 weeks previously ($n = 20$ mice) were processed and stained with hematoxylin and eosin.

RT-PCR. Reverse transcription-PCR (RT-PCR) and a previously published (36) competitive semiquantitative PCR were used to detect the viral genome as described below. Total RNA was extracted from the brain and spinal cord, separately, using an Ultraspec II RNA isolation system (Biotecx Laboratories, Inc., Houston, Tex.) in accordance with the manufacturer's directions. RT was performed in a total volume of 30 μl at 37°C for 90 min with 300 U of Super-Script II Moloney murine leukemia virus RNase H$^-$ reverse transcriptase (GIBCO, Grand Island, N.Y.), first-strand buffer (50 mM Tris-HCl [pH 8.3], 75 mM KCl, 3 mM $MgCl_2$), 10 mM dithiothreitol, 2 mM each deoxynucleoside triphosphate, 3 μl of a 50-μg/ml solution of random hexamer primers (Promega, Madison, Wis.), and 5 μg of the extracted RNA. The solution was then heated at 95°C for 10 min, and 120 μl of distilled H_2O was added. Adjusted amounts of the test cDNAs were then amplified with DA-specific primers that have been previously described (36). The PCR was performed in a total volume of 100 μl containing 3 μl of the cDNA generated in the RT reaction, 10× PCR buffer (10 mM Tris-HCl [pH 8.3], 50 mM KCl, 1.5 mM $MgCl_2$), 40 pmol of each primer, 2 mM each deoxynucleoside triphosphate, and 0.5 μl of AmpliTaq DNA polymerase (5 U/μl; Perkin-Elmer Cetus, Norwalk, Conn.). In the case of the competitive RT-PCR, the PCR was performed in the presence of a recombinant clone, pDALAPP (42), which contains an insertion in the L coding region of pDAFL3 (so that the amplified pDALAPP product has a slower electrophoretic mobility than the wild-type DA product). As previously described (36), the PCR mixture contained an amount of competitor cDNA sufficient to register an appropriate signal of the test cDNA and an amount of test cDNA, in 3 to 5 μl of the RT reaction solution, adjusted to contain a quantity of hypoxanthine phosphoribosyltransferase cDNA similar to that of companion specimens. The PCR conditions were as follows: 1 cycle of 94°C for 3 min; 35 to 45 cycles of 94°C for 45 s (52 s for hypoxanthine phosphoribosyltransferase), 60°C (for the DA cDNA) for 15 s, and 72°C for 45 s; and 1 cycle of 72°C for 5 min. Aliquots of the PCR products were electrophoresed in 2.5% agarose gels and stained with 1% ethidium bromide.

RESULTS

DA virus with a mutation in L* grows in various cell types. To determine whether L* affects the ability of DA to grow in various tissue culture cells, we compared the growth of wild-type DA virus and DAL*-1 virus (whose genome maps are shown in Fig. 1) in BHK-21 cells and P388D1 cells. The two viruses had similar one-step growth curves in BHK-21 cells (Fig. 2) and similar titers at 8 and 16 to 18 h after infection of P388D1 cells (Table 1).

DA L* prevents premature shutoff of host cell protein synthesis. To examine the effect of L* on DA virus infection of different cell types, we radiolabeled BHK-21 and P388D1 cells infected with wild-type DA virus or DAL*-1 virus. As expected,

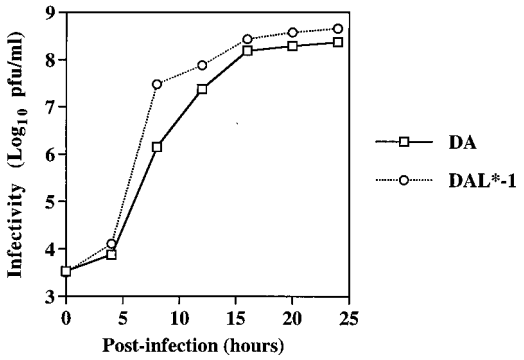

FIG. 2. One-step growth curves of wild-type DA and DAL*-1 virus in BHK-21 cells.

wild-type DA virus infection of cells led to the synthesis of viral proteins and a progressive shutoff of host cell protein translation in a permissive cell line, BHK-21 (Fig. 3, lanes 4, 10, and 16). Similar findings with respect to the synthesis of viral proteins and the shutoff of cellular proteins were obtained following DAL*-1 virus infection of BHK-21 cells (Fig. 3, lanes 5, 11, and 17).

As in the case with BHK-21 cells, DA wild-type virus infection of P388D1 cells led to the synthesis of viral proteins followed by a progressive decline in cellular protein synthesis (Fig. 3, lanes 1, 7, and 13). The radiolabeled L* band indicated that a significant amount of L* protein was synthesized by wild-type virus in both BHK-21 and P388D1 cells (Fig. 3). As calculated with a PhosphorImager, the ratio of L* to VP3 in P388D1 cells was 0.4 times that in BHK-21 cells, suggesting that different cell types vary in their utilization of the L*-initiating AUG versus the polyprotein's initiating AUG.

We then examined radiolabeled viral and cellular proteins following infection of P388D1 cells with DAL*-1 virus. DAL*-1 virus had an apparently premature shutoff of synthesis of both viral and host cell proteins. There was a much greater inhibition of host cell protein synthesis in P388D1 cells after infection with DAL*-1 (Fig. 3C, lane 14) than after DA wild-type virus infection (lane 13) at 10 to 18 h p.i., a time when there was relatively less synthesis of viral proteins by the mutant than by the wild-type virus. This finding was a consistent one, as shown by the results of a different experiment (Fig. 3D, lanes 19 and 20). The differences in inhibition of host cell protein synthesis were not a result of differences in the wild-type and mutant virus MOIs, since similar results were obtained with different stocks of virus used at the same MOI (data not shown) and because the results were cell type specific (i.e., the changes observed in P388D1 cells were not seen in BHK-21 cells). The changes were also seen in J774.1 mouse macrophage cells and after infection with DA viruses that contained various mutations of L* (data not shown).

DA L* inhibits virus-induced apoptosis of P388D1 cells. The shutoff of both viral and host cell protein synthesis following P388D1 cell infection with DAL* mutant viruses suggested that the infection might have induced apoptosis of the cells. To investigate this possibility, we used ethidium bromide staining of agarose gels to examine infected P388D1 cells for evidence

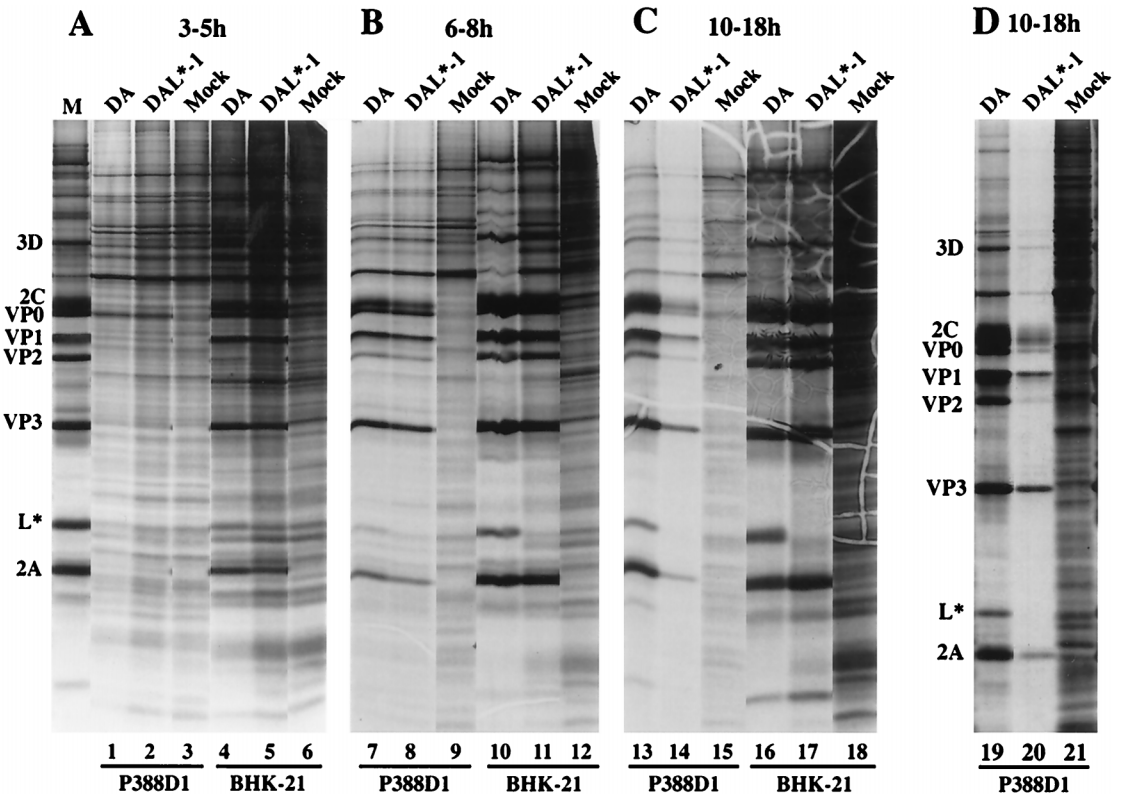

FIG. 3. DAL*-1 virus infection of P388D1 cells causes a premature shutoff of viral and cellular protein synthesis. Shown is an autoradiogram of P388D1 and BHK-21 cells that were either mock infected or infected with wild-type DA or DAL*-1 virus and then radiolabeled at 3 to 5 h p.i. (A), 6 to 8 h p.i. (B), or 10 to 18 h p.i. (C and D). Cells were harvested at the end of the period of radiolabeling. M, the left-most lane in panel A, is a marker lane for the viral proteins and contains radiolabeled BHK-21 cells infected with DA virus.

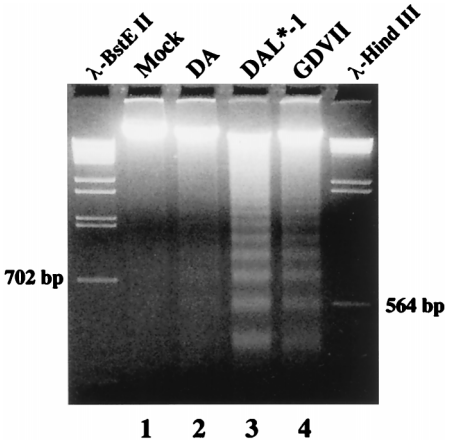

FIG. 4. DAL*-1 or GDVII virus infection of P388D1 cells induces DNA laddering. Prominent DNA laddering is seen with DAL*-1 (lane 3) and GDVII (lane 4) virus infections, but little is seen with wild-type DA virus infection (lane 2) and none is evident with mock infection (lane 1). Marker lanes show λ DNA following digestion with *BstE*II or *Hin*dIII.

of DNA fragmentation. Figure 4 shows that 12 h after infection with DAL*-1 (lane 3) or GDVII (lane 4) virus there was evidence of DNA laddering that was not seen in the mock-infected (lane 1) or wild-type DA virus-infected (lane 2) P388D1 cells or with infection of BHK-21 cells (data not shown) by these viruses. The apoptotic nature of the cell death was confirmed by Hoechst 33342 staining (Fig. 5A to D), which revealed extensive nuclear condensation and the presence of apoptotic bodies following infection with DAL*-1 (Fig. 5C) and GDVII (Fig. 5D) viruses which was rarely seen in mock-infected cells (Fig. 5A) or after wild-type DA infection (Fig. 5B).

To quantitate the apoptosis, we examined TUNEL-stained P388D1 cells following mock infection or infection with wild-type DA, DAL*-1, or GDVII virus. Figure 5E to I show the results of a representative experiment in which apoptosis was apparent at 12 h following infection with DAL*-1 virus (Fig. 5G and I) (38% of the cells were apoptotic) or GDVII virus (Fig. 5H and I) (43%), while there was little apoptosis evident at 12 h following wild-type DA virus infection (Fig. 5F and I) (6%) or mock infection (Fig. 5E and I) (1%). Although the number of TUNEL-positive cells increased at 16 h after infection (Fig. 5I) with wild-type DA virus (when the apoptosis value was approximately 40%), the degree of apoptosis was significantly less ($P < 0.01$) than that seen following DAL*-1 or GDVII virus infection (for which the value was over 85% at 16 h p.i.). In addition, the level of apoptosis seen in P388D1 cells at 16 h after infection with wild-type DA virus was actually probably less than 40%, since many cells had already died of a nonapoptotic virus-induced cell lysis. An evaluation of the cells at 16 h p.i. was not possible because of extensive cell death from lysis. Similar results were obtained with BSC-1 cells (data not shown), a relatively nonpermissive cell line in which GDVII virus has been reported to be far more effective at inducing apoptosis than BeAn virus (which is a TO subgroup strain similar to DA virus) (11). There was little evidence of apoptosis (<5%) following infection of BHK-21 cells with each of these viruses, even at 24 h p.i., at which time the cells began to lyse.

These results suggest that all three viruses have some apoptotic effect but that DAL*-1 has a much more pronounced apoptotic effect than wild-type DA virus. Since the only difference in the proteins produced following wild-type DA and DAL*-1 virus infection is the synthesis of L* by the former, we presume that the reduced apoptosis in wild-type DA virus-infected P388D1 cells is attributed to an antiapoptotic effect of L*. The increased apoptosis seen following infection with GDVII virus compared to that evident with DA is presumably at least partly related to the absence of L* synthesis (since GDVII virus lacks the L* AUG).

DA L* is important for persistence of virus within the CNS. Our previous published studies showed that virus with a mutation in L* was no longer able to induce a late demyelinating disease (7). To clarify whether this failure was a result of the inability of the mutant virus to grow well in the CNS, we compared the pathologies and amounts of virus and viral genome in the CNS of animals following infection with wild-type or DAL*-1 virus.

DAL*-1 virus produced an early acute polioencephalomyelitis that was not dissimilar to that seen with wild-type virus (Fig. 6). Seven days after infection with wild-type DA or DAL*-1 virus, destructive lesions and inflammatory infiltrates were frequently seen in the hippocampus (Fig. 6A and B, respectively) and neuronophagia and inflammatory cells in the anterior horns and anterior root exit zones (Fig. 6C and D, respectively). In addition, levels of virus in the brain and spinal cord were similar 7 days after infection with DA or DAL*-1 virus (Table 1). These results demonstrated that DAL*-1 virus (which fails to synthesize L*) is acutely pathogenic at 1 week p.i. and that within the CNS it replicates as well as the wild-type virus. Therefore, the absence of DAL*-1 virus persistence at 6 weeks p.i. cannot be explained by an absence of early disease.

We next wondered whether the inability of DAL*-1 virus to induce demyelinating disease is due to the failure of this mutant virus to persist, since the demyelinating disease must be accompanied by virus persistence (32). Since the level of infectious DA virus is generally very low at the time of occurrence of the demyelinating disease, we performed RT-PCR on RNA extracted from the spinal cords of infected mice. A competitive semiquantitative RT-PCR showed that the viral genome was easily detectable and that its levels in the mouse brain and spinal cord were comparable 1 week after infection with wild-type or DAL*-1 virus (Fig. 7A, Brain 1w and SC 1w, respectively); i.e., the RNA from at least two of three animals infected with DAL*-1 had a lower band, corresponding to the viral genome, that was similar in intensity to the lower band of the viral genome from animals inoculated with DA. At 6 weeks p.i., the viral genome was present, as determined by competitive RT-PCR, in the spinal cords of mice infected with wild-type virus (Fig. 7A, SC 6w, DA); however, there was no detectable amplified viral genome product in the spinal cords of mice inoculated with DAL*-1 virus (and only the upper band, corresponding to the larger, amplified pDAL product, is seen) (Fig. 7A, SC 6w, L*-1). A standard RT-PCR confirmed these findings, demonstrating that the viral genome was present in the brain and spinal cord 1 week after infection with DAL*-1 virus (Fig. 7B, Brain 1W and SC 1w, respectively), but no signal could be detected 6 weeks after infection with DAL*-1 virus (Fig. 7B, SC 6w); in contrast, the viral genome was present in the CNS at 1 and 6 weeks after infection with wild-type DA virus. As expected from our previously published results (7), there was little if any demyelination or pathology in animals inoculated with DAL*-1 virus, while extensive inflammatory demyelination was evident in the spinal cords of mice inoculated with wild-type virus (data not shown). These data indicate that DA L* is critically important for virus persistence and suggest that DAL*-1 virus fails to demyelinate because of the inability of the virus to persist.

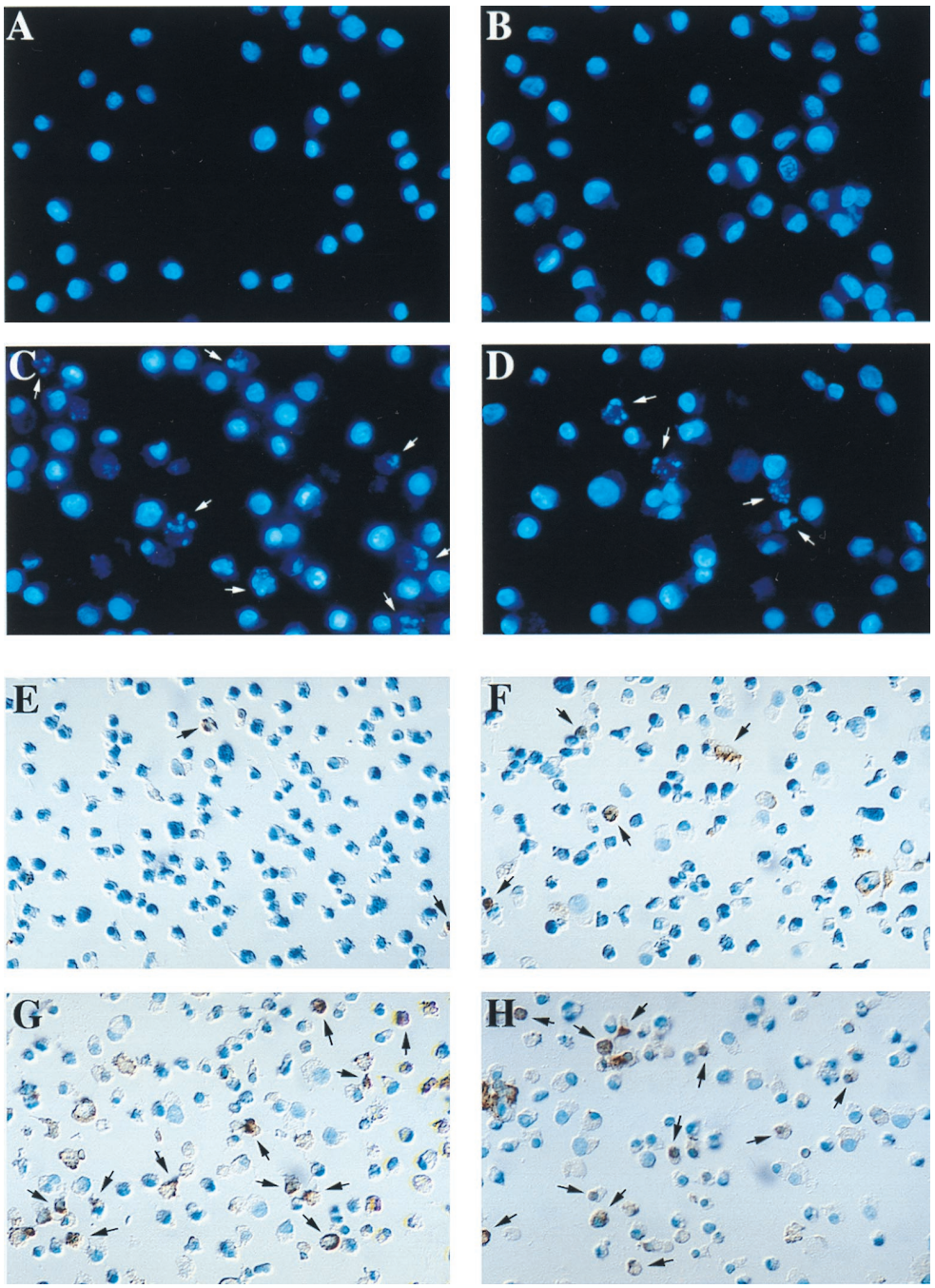

FIG. 5. DAL*-1 or GDVII virus infection of P388D1 cells induces fragmentation of chromatin and double-stranded DNA breaks. Hoechst 33342 staining shows chromatin fragmentation (arrows) in P388D1 cells 12 h following DAL*-1 (C) or GDVII (D) virus infection, but this was not evident in mock-infected (A) or wild-type DA-infected (B) cells. TUNEL staining of P388D1 cells is seen 12 h following DAL*-1 (G) or GDVII (H) virus infection, but it was not evident in mock-infected (E) or wild-type DA-infected (F) cells. (I) Histogram of the percentages of TUNEL-positive cells (mean ± standard error of the mean) at 12 and 16 h p.i. This representative experiment was determined from enumeration of cells in five to seven different microscope fields of three to four coverslips.

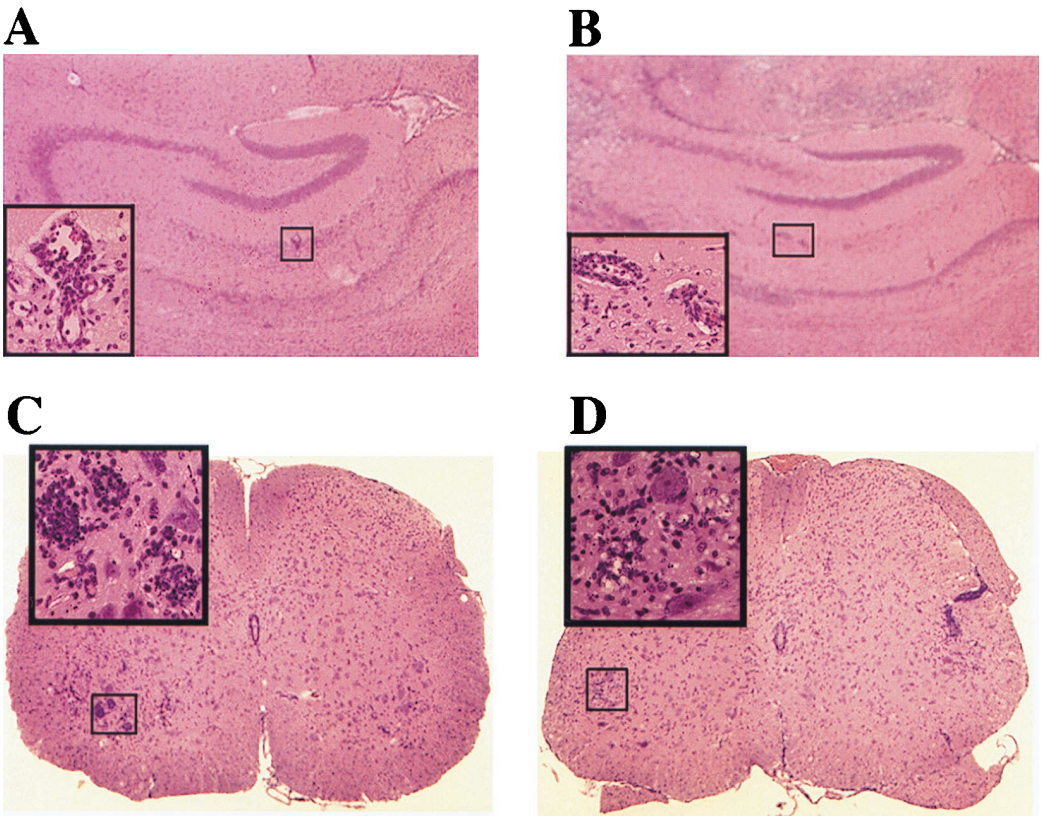

FIG. 6. DA and DAL*-1 viruses induce gray matter pathology in the CNS by 1 week p.i. Shown are sections of the hippocampus (A and B) and the spinal cord (C and D) from mice infected with wild-type DA virus (A and C) or DAL*-1 virus (B and D). The large inset in each panel is a higher magnification of the smaller highlighted rectangle. Areas of inflammation are shown in the insets in panels A and C. The insets in panels B and D show regions of neuronophagia in the anterior horn.

DISCUSSION

DA and other TO subgroup strains of TMEV induce a biphasic disease with an initial subclinical gray matter neuronal infection followed by a chronic demyelination. Virus persists, with restricted expression, in microglia, oligodendrocytes, and astrocytes in the spinal cord. In contrast, GDVII strains and members of the GDVII subgroup of TMEV induce an acute fatal gray matter disease with no evidence of demyelination or virus persistence. The phenotype of TO subgroup strains is of interest because persistence and the nonlytic restricted expression of a picornavirus are distinctly unusual and because TO subgroup-induced demyelinating disease provides an excellent experimental model of MS.

We were initially interested in clarifying the role of L* because the L* initiation codon is present in TO subgroup strains but not in GDVII subgroup strains, suggesting that this protein product might be important in TO subgroup virus-induced demyelination and persistence. Of special note were findings from our original DA sequencing study (26) which demonstrated that among TMEV strains there is greater conservation of the L coding region, which is the upstream-most part of the polyprotein's coding region and from which L* is initiated and partly synthesized, at the nucleotide level than at the amino acid level. In addition, there are between 9 and 11 amino acid mismatches when TO subgroup strains DA and BeAn L are compared, and there are 11 such mismatches evident when DA and GDVII L proteins are compared. In contrast, there are only 6 amino acid mismatches when the first 76 amino acids of DA and BeAn L* (equivalent to the size of L) are compared, and there are 8 such mismatches when the first 76 amino acids of DA and GDVII L* are compared. In other words, the difference in the amino acid sequences of L among different TMEV strains is greater than the difference in the amino acid sequences of the corresponding region of L* among these strains. These findings suggest that TMEV strains have been under selection pressure to maintain the third codon, presumably in order to maintain the alternative reading frame of L*. The importance of L* was confirmed in later studies that showed that L* is synthesized both in vitro as well as in infected cells (7, 15) and that L* is critical for the production of the demyelinating disease (7). The present demonstration that a significant amount of L* protein is synthesized during infections in BHK-21 cells again suggests an important role for this protein.

Our results showed that the growth and behavior of DA L* mutant virus depend on the cell type infected. DAL*-1 virus,

TABLE 1. Virus levels in P388D1 cells, brain, and spinal cord after infection with DA or DAL*-1

Infecting virus	Virus yield[a] (log_{10}) in:			
	P388D1 cells		Brain (at 1 wk p.i.)	Spinal cord (at 1 wk p.i.)
	At 8 h p.i.	At 16 to 18 h p.i.		
DA	5.87 ± 0.66	5.62 ± 0.37	4.61 ± 0.3	3.71 ± 0.22
DAL*-1	5.82 ± 0.74	5.28 ± 0.46	4.44 ± 0.39	3.87 ± 0.56

[a] Virus yields for P388D1 cells are in PFU per milliliter; those for brain and spinal cord are in PFU per gram of tissue.

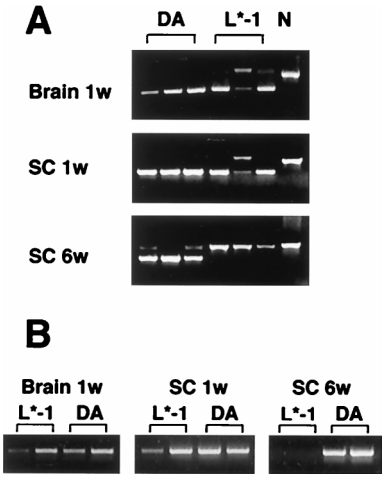

FIG. 7. DAL*-1 virus and wild-type DA virus induce similar amounts of viral genome in the CNS early after infection, but the genome of the former does not persist. (A) Semiquantitative RT-PCR of RNA extracted from the brains and spinal cords (SC) of mice inoculated 1 week (1w) or 6 weeks (6w) after infection with wild-type (DA) or DAL*-1 (L*-1) virus or of an uninoculated mouse (N). Each lane represents brain or spinal cord from an individual mouse. The uppermost band on each of the gels shows the position of the competitor pDAL, which has a slower mobility than the lower band, which represents the DA genome in the CNS specimen. Only one band corresponding to the competitor pDAL is seen in some lanes because there is no detectable viral genome in the brain or spinal cord specimen. (B) RT-PCR of RNA extracted from the brains and spinal cords of mice inoculated 1 or 6 weeks after infection with DA or L*-1 virus.

which is unable to synthesize L*, grew well in cells that are very permissive for DA strain infection, such as BHK-21 cells. In addition, DAL*-1 virus induced an acute gray matter infection similar to that seen with wild-type virus infection, and with comparable levels of virus. In contrast, there were remarkable differences in the growth and behavior of the wild-type and DAL*-1 viruses following infection of mouse macrophage cells. Infection of P388D1 cells with DAL*-1 virus induced a shutoff of host cell protein synthesis at a time when viral protein production had not reached as high a level as was associated with host cell shutoff in wild-type virus infection. Further studies showed that the reason for this premature inhibition of cellular protein synthesis was the induction of apoptosis in P388D1 cells. Although there was evidence of apoptosis following infection with DA, the apoptosis seen following infection with DA L* mutant virus occurred earlier and was significantly more prominent. The results suggested that the L* protein inhibits and slows down the apoptotic cell death that is induced in certain cell types following TMEV infection. The degree of virus-induced apoptosis in a cell type may depend on the apoptosis "machinery" that is present in that cell type and also the amount of L* that is synthesized in the cell (i.e., how much translation initiation occurs from the AUG codon at N1079 and how much takes place from the AUG codon at N1066).

Apoptosis has been previously reported in the case of infections with picornaviruses, including TMEV (11). Tolskaya et al. (39) found that poliovirus infection induces apoptosis, as well as antiapoptosis, in certain cells under nonpermissive conditions. Jelachich and Lipton (11) reported that TMEV induces apoptosis under restrictive conditions, with GDVII virus inducing at least 50-fold more apoptosis than BeAn following infection of BSC-1 cells, a nonpermissive cell line. In addition, Tsunoda et al. (40) described the occurrence of a greater extent of apoptosis in neurons and microglia in the mouse CNS early after infection with GDVII than following DA infection. Our data suggest that the higher level of apoptotic activity reported with strain GDVII than that evident after infection with a TO subsgroup strain is at least partly related to the absence of an L* initiation codon in the GDVII genome (and therefore the absence of L* synthesis in GDVII virus infections). Obuchi et al. (25) recently reported that the GDVII strain does not actively replicate in J774-1 mouse macrophages despite a significant inhibition of cellular protein synthesis; in contrast, the DA strain grows well in these cells. The results of the present study suggest that the inoculation of J774-1 cells with the GDVII strain results in less infectious virus than does inoculation with the DA strain because GDVII triggers a more prominent apoptosis in these cells.

Our study demonstrated that L* is important in mediating virus persistence. This may occur through an interference with the anti-TMEV cytolytic T-cell response, since that response is absent in mouse strains that are susceptible to the late demyelinating disease following infection with the wild-type virus, presumably preventing virus clearance (17, 18, 29). Recent studies have demonstrated that this is the case and that L* inhibits the cytolytic T-cell response 7 days p.i.; i.e., mouse strains which are normally susceptible to demyelination, normally have high levels of infectious virus in the CNS (Table 1), and normally fail to generate a virus-specific cytolytic T-cell response following wild-type DA virus infection do induce a virus-specific cytolytic T-cell response following DAL*-1 virus infection (16a). The generation of this virus-specific cytolytic T-cell response following DAL*-1 virus infection presumably leads to virus clearance and prevents demyelination from occurring (since virus persistence has been found to be necessary for the white matter disease [32]).

It may be that the antiapoptotic activity of L* plays a key role in inhibiting this virus-specific cytolytic T-cell response, since apoptosis has been implicated in the induction of this response (1) and because the cytolytic T-cell response is believed to involve apoptotic pathways. A direct inhibition of the cytolytic T-cell response could occur, as has been described in the case of two orthopoxvirus antiapoptotic proteins that are members of the serpin family of protease inhibitors (20, 21). Another possibility is that L* inhibits apoptosis of macrophages, thereby allowing widespread infection of these cells, with the subsequent elimination of these antigen-presenting cells at a time critical for effective virus clearance by the cytolytic T-cell response.

An increased utilization of the L* AUG by ribosomes for translation initiation and a decreased initiation of translation at the polyprotein's AUG may limit the production of capsid protein, the target for the cytolytic T-cell response (17). This relative decrease in synthesis of capsid proteins not only may prevent the generation of a cytolytic T-cell response but may also favor restricted virus expression. It may be that there is a greater degree of initiation of L* translation at nt 1079 in microglia (which are the major reservoir of virus during the persistent CNS infection [19] and which have a restricted infection) than in BHK-21 cells and neurons (i.e., productively infected cells), perhaps because cell-specific proteins bind the viral genome. In this way, a cell type-specific regulation of two different initiation codons for translation can increase the synthesis of either L* (and lead to an inhibition of virus-induced apoptosis, an inhibition of a virus-specific cytolytic T-cell response, and restricted virus expression because of a decrease in viral capsid protein synthesis) or the polyprotein and capsid proteins.

It is now recognized that apoptosis can play an important role in viral infections (31) and, in addition, can disturb the immune system balance, thereby contributing to autoimmune processes (27). A number of investigations have demonstrated that induction of apoptosis of T cells and macrophages by

various mechanisms (e.g., encephalitogenic proteins, peptides, and steroids) alleviates acute experimental allergic encephalomyelitis (EAE) (23, 24, 28), an experimental model of MS. In addition, apoptosis of T cells during recovery from acute EAE and in brain infiltrates in chronic EAE has been reported (22), suggesting that an inhibition of apoptosis may enhance immune-mediated demyelination and limit recovery (14); some studies, however, suggested that an inhibition of apoptosis may result in protection against EAE (34, 41). In an analogous way, there is accumulating evidence that resolution of an attack of MS is related to apoptotic activity. Steroids, which induce apoptosis of T cells (37), alleviate MS as well as EAE. Recent studies of affected CNS regions (8) and T cells (10) of MS patients describe abnormalities of the apoptotic pathway. Our studies indicate a role for apoptosis in a chronic inflammatory demyelinating disease and, by analogy, suggest that regulation of apoptosis may also be important in MS disease pathogenesis.

ACKNOWLEDGMENTS

G.D.G. and L.M. contributed equally to this study.

This work was supported by grants from the National Multiple Sclerosis Society and the National Institutes of Health.

REFERENCES

1. **Albert, M. L., B. Sauter, and N. Bhardwaj.** 1998. Dendritic cells acquire antigen from apoptotic cells and induce class I-restricted CTLs. Nature **392:**86–89.
2. **Aubert, C., M. Chamorro, and M. Brahic.** 1987. Identification of Theiler's virus infected cells in the central nervous system of the mouse during demyelinating disease. Microb. Pathog. **3:**319–326.
3. **Bose, R., M. Verheij, A. Haimovitz-Friedman, K. Scotto, Z. Fuks, and R. Kolesnick.** 1995. Ceramide synthase mediates daunorubicin-induced apoptosis: an alternative mechanism for generating death signals. Cell **82:**405–414.
4. **Cash, E., M. Chamorro, and M. Brahic.** 1988. Minus-strand RNA synthesis in the spinal cords of mice persistently infected with Theiler's virus. J. Virol. **62:**1824–1826.
5. **Cash, E., M. Chamorro, and M. Brahic.** 1986. Quantitation, with a new assay, of Theiler's virus capsid protein in the central nervous system of mice. J. Virol. **60:**558–563.
6. **Cash, E., M. Chamorro, and M. Brahic.** 1985. Theiler's virus RNA and protein synthesis in the central nervous system of demyelinating mice. Virology **144:**290–294.
7. **Chen, H. H., W. P. Kong, L. Zhang, P. L. Ward, and R. P. Roos.** 1995. A picornaviral protein synthesized out of frame with the polyprotein plays a key role in a virus-induced immune-mediated demyelinating disease. Nat. Med. **1:**927–931.
8. **D'Souza, S. D., B. Bonetti, V. Balasingam, N. R. Cashman, P. A. Barker, A. B. Troutt, C. S. Raine, and J. P. Antel.** 1996. Multiple sclerosis: Fas signaling in oligodendrocyte cell death. J. Exp. Med. **184:**2361–2370.
9. **Fu, J. L., S. Stein, L. Rosenstein, T. Bodwell, M. Routbort, B. L. Semler, and R. P. Roos.** 1990. Neurovirulence determinants of genetically engineered Theiler viruses. Proc. Natl. Acad. Sci. USA **87:**4125–4129.
10. **Ichikawa, H., K. Ota, and M. Iwata.** 1996. Increased Fas antigen on T cells in multiple sclerosis. J. Neuroimmunol. **71:**125–129.
11. **Jelachich, M. L., and H. L. Lipton.** 1996. Theiler's murine encephalomyelitis virus kills restrictive but not permissive cells by apoptosis. J. Virol. **70:**6856–6861.
12. **Jordan, J., M. F. Galindo, J. H. Prehn, R. R. Weichselbaum, M. Beckett, G. D. Ghadge, R. P. Roos, J. M. Leiden, and R. J. Miller.** 1997. p53 expression induces apoptosis in hippocampal pyramidal neuron cultures. J. Neurosci. **17:**1397–1405.
13. **Kaminski, A., M. T. Howell, and R. J. Jackson.** 1990. Initiation of encephalomyocarditis virus RNA translation: the authentic initiation site is not selected by a scanning mechanism. EMBO J. **9:**3753–3759.
14. **Karlik, S. J., S. Hyduk, and H. Horner.** 1996. Apoptosis throughout chronic EAE. Multiple Sclerosis Clin. Lab. Res. **2:**249.
15. **Kong, W.-P., and R. P. Roos.** 1991. Alternative translation initiation site in the DA strain of Theiler's murine encephalomyelitis virus. J. Virol. **65:**3395–3399.
16. **Levy, M., C. Aubert, and M. Brahic.** 1992. Theiler's virus replication in brain macrophages cultured in vitro. J. Virol. **66:**3188–3193.

16a. **Lin, X., R. P. Roos, L. Pease, P. Wettstein, and M. Rodriguez.** A Theiler's virus alternatively initiated protein inhibits the generation of H-2K-restricted virus-specific toxicity. Submitted for publication.

17. **Lin, X., N. R. Thiemann, L. R. Pease, and M. Rodriguez.** 1995. VP1 and VP2 capsid proteins of Theiler's virus are targets of H-2D-restricted cytotoxic lymphocytes in the central nervous system of B10 mice. Virology **214:**91–99.
18. **Lindsley, M. D., R. Thiemann, and M. Rodriguez.** 1991. Cytotoxic T cells isolated from the central nervous systems of mice infected with Theiler's virus. J. Virol. **65:**6612–6620.
19. **Lipton, H. L., G. Twaddle, and M. L. Jelachich.** 1995. The predominant virus antigen burden is present in macrophages in Theiler's murine encephalomyelitis virus-induced demyelinating disease. J. Virol. **69:**2525–2533.
20. **Macen, J. L., R. S. Garner, P. Y. Musy, M. A. Brooks, P. C. Turner, R. W. Moyer, G. McFadden, and R. C. Bleackley.** 1996. Differential inhibition of the Fas- and granule-mediated cytolysis pathways by the orthopoxvirus cytokine response modifier A/SPI-2 and SPI-1 protein. Proc. Natl. Acad. Sci. USA **93:**9108–9113.
21. **Macen, J. L., K. A. Graham, S. F. Lee, M. Schreiber, L. K. Boshkov, and G. McFadden.** 1996. Expression of the myxoma virus tumor necrosis factor receptor homologue and M11L genes is required to prevent virus-induced apoptosis in infected rabbit T lymphocytes. Virology **218:**232–237.
22. **McCombe, P. A., I. Nickson, Z. Tabi, and M. P. Pender.** 1996. Apoptosis of Vβ 8.2+ T lymphocytes in the spinal cord during recovery from experimental autoimmune encephalomyelitis induced in Lewis rats by inoculation with myelin basic protein. J. Neurol. Sci. **139:**1–6.
23. **McFarland, H. I., J. M. Critchfield, M. K. Racke, J. P. Mueller, S. H. Nye, S. A. Boehme, and M. J. Lenardo.** 1995. Amelioration of autoimmune reactions by antigen-induced apoptosis of T cells. Adv. Exp. Med. Biol. **383:**157–166.
24. **Nguyen, K. B., P. A. McCombe, and M. P. Pender.** 1994. Macrophage apoptosis in the central nervous system in experimental autoimmune encephalomyelitis. J. Autoimmun. **7:**145–152.
25. **Obuchi, M., Y. Ohara, T. Takegami, T. Murayama, H. Takada, and H. Iizuka.** 1997. Theiler's murine encephalomyelitis virus subgroup strain-specific infection in a murine macrophage-like cell line. J. Virol. **71:**729–733.
26. **Ohara, Y., S. Stein, J. L. Fu, L. Stillman, L. Klaman, and R. P. Roos.** 1988. Molecular cloning and sequence determination of DA strain of Theiler's murine encephalomyelitis viruses. Virology **164:**245–255.
27. **Osborne, B. A.** 1996. Apoptosis and maintenance of homeostasis in the immune system. Curr. Opin. Immunol. **8:**245–254.
28. **Pearson, C. I., W. van Ewijk, and H. O. McDevitt.** 1997. Induction of apoptosis and T helper 2 (Th2) responses correlates with peptide affinity for the major histocompatibility complex in self-reactive T cell receptor transgenic mice. J. Exp. Med. **185:**583–599.
29. **Pena Rossi, C., A. McAllister, L. Fiette, and M. Brahic.** 1991. Theiler's virus infection induces a specific cytotoxic T lymphocyte response. Cell. Immunol. **138:**341–348.
30. **Qi, Y., and M. C. Dal Canto.** 1996. Effect of Theiler's murine encephalomyelitis virus and cytokines on cultured oligodendrocytes and astrocytes. J. Neurosci. Res. **45:**364–374.
31. **Razvi, E. S., and R. M. Welsh.** 1995. Apoptosis in viral infections. Adv. Virus Res. **45:**1–60.
32. **Roos, R. P., and N. Casteel.** 1992. Determinants of neurological disease induced by Theiler's murine encephalomyelitis virus, p. 283–318. *In* R. P. Roos (ed.), Molecular neurovirology. Humana Press, Totowa, N.J.
33. **Roos, R. P., S. Stein, Y. Ohara, J. Fu, and B. L. Semler.** 1989. Infectious cDNA clones of the DA strain of Theiler's murine encephalomyelitis virus. J. Virol. **63:**5492–5496.
34. **Sabelko, K. A., K. A. Kelly, M. H. Nahm, A. H. Cross, and J. H. Russell.** 1997. Fas and Fas ligand enhance the pathogenesis of experimental allergic encephalomyelitis, but are not essential for immune privilege in the central nervous system. J. Immunol. **159:**3096–3099.
35. **Sangar, D. V., S. E. Newton, D. J. Rowlands, and B. E. Clarke.** 1987. All foot and mouth disease virus serotypes initiate protein synthesis at two separate AUGs. Nucleic Acids Res. **15:**3305–3315.
36. **Sato, S., S. L. Reiner, M. A. Jensen, and R. P. Roos.** 1997. Central nervous system cytokine mRNA expression following Theiler's murine encephalomyelitis virus infection. J. Neuroimmunol. **76:**213–233.
37. **Sun, X. M., D. Dinsdale, R. T. Snowden, G. M. Cohen, and D. N. Skilleter.** 1992. Characterization of apoptosis in thymocytes isolated from dexamethasone-treated rats. Biochem. Pharmacol. **44:**2131–2137.
38. **Tesar, M., S. A. Harmon, D. F. Summers, and E. Ehrenfeld.** 1992. Hepatitis A virus polyprotein synthesis initiates from two alternative AUG codons. Virology **186:**609–618.
39. **Tolskaya, E. A., L. I. Romanova, M. S. Kolesnikova, T. A. Ivannikova, E. A. Smirnova, N. T. Raikhlin, and V. I. Agol.** 1995. Apoptosis-inducing and apoptosis-preventing functions of poliovirus. J. Virol. **69:**1181–1189.
40. **Tsunoda, I., G. I. B. Kurtz, and R. S. Fujinami.** 1997. Apoptosis in acute and chronic central nervous system disease induced by Theiler's murine encephalomyelitis virus. Virology **228:**388–393.
41. **Waldner, H., R. A. Sobel, E. Howard, and V. K. Kuchroo.** 1997. Fas- and FasL-deficient mice are resistant to induction of autoimmune encephalomyelitis. J. Immunol. **159:**3100–3103.
42. **Zhang, L., S. Sato, J. I. Kim, and R. P. Roos.** 1995. Theiler's virus as a vector for foreign gene delivery. J. Virol. **69:**3171–3175.